TR-PIV measurements in open channel flow for the analysis of undular tidal bores

L. David[1*], L. Chatellier[1], D. Calluaud[1], Y. J. Jeon[1], G. Rousseaux[1], L. Thomas[1]

1: Institut Pprime, CNRS, Université de Poitiers, ENSMA, France
* Correspondent author: Laurent.David@univ-poitiers.fr

Abstract: For several years, tidal bores have been the object of many investigations but some aspects remain always unknown. In this paper, we generate such type of flow in a laboratory to investigate, with classical measurement tools associated to optical diagnostics, the influence of different parameters as the water depth, the upstream velocity and initial conditions of boundary layer. Different kinds of moving bores have been generated for one Froude number Fr=1.29 and three initial boundary layer conditions. The water depth evolution doesn't seem to be affected by the boundary-layer conditions while the internal flow is significantly altered during the passage of the whelps depending on these conditions. For the first time, the velocity field evolution is shown inside the water column.

1. Introduction

The tidal bore is a natural and powerful phenomenon that forms in rivers as the tidal flow turns to rising. It is characterized by a brutal rise of water level followed by series of waves propagating upstream for kilometers. For several years, this phenomenon has been studied from different points of view. The Froude number Fr based on the upstream velocity V_1, the celerity of the bore U for an observer placed on the ground and the water depth h_1 allows the classification of tidal bores in three different types (Chanson and Docherty, 2012). For the range of Fr between 1 and 1.25-1.3, the bore has an undular wave pattern. It propagates upstream relatively slowly and the front is followed by a suite of well-formed whelps. For Fr between 1.3 and 1.5, an undular bore with some slight wave breaking is present and for Froude numbers greater than 1.5, breaking bores appear with a more marked roller. Some theoretical approaches have tried to characterize the height ratio between the upstream water depth and the mean water depth just after the passage of the bore but also the amplitude and shape of the waves propagating with the bore (Barré de Saint-Venant, 1871, Lemoine, 1948, Benjamin and Lighthill, 1954, Chanson, 2010). Field measurements have shown that the different kinds of bores exist and that the streamwise velocity and the turbulence intensity are highly modified just downstream the arrival of the bore (Tessier and Terwindt, 1994, Wolanski et al., 2004, Huang et al, 2013, Xie and Pan, 2013). Laboratory measurements are in this case very useful to get some more controlled experiments of this phenomenon and give the opportunity to master different parameters like the flow discharge, the water depth, the bed roughness, and the upstream mean flow conditions. These studies have been carried out essentially by means of water depth and single-point velocity measurements using Pitot-tubes or Acoustic Doppler Velocimeters (Koch and Chanson, 2009, Chanson, 2011, Chanson and Docherty, 2012, Huang et al, 2013) but also with PIV measurements (Hornung et al, 1995, David et al, 2014). Finally numerical simulations by 1D shallow water equation (Jian S et al., 2014) or by Large Eddy Simulation (Lubin et al, 2010) confirmed the water depth evolution, highlighted the occurrence of these turbulent events and showed the production of vorticity behind the bore front, whose large scale structures stay at the bottom of the channel.

The knowledge of tidal bores stays incomplete and laboratory experiments are still necessary to better understand the wave propagation inside the water column for comparing with numerical simulations. In this paper, time-resolved PIV measurements in an open channel are carried out to study the undular tidal bore close to the transition between two states (Fr=1.29) in laboratory conditions. The main encountered experimental difficulties to record and to analyze a flow with free surface will be discussed first. In a second part, the influence of the initial flow boundary conditions on the free surface evolution will be addressed, and finally the effect of the different conditions will be studied during the passage of the bore.

2.Experimental devices and data processing

2.1 Tidal bore description

A tidal bore is a positive surge travelling upstream, it is also called a hydraulic jump in translation. If one moves with the bore, i.e the hydraulic jump is fixed in a translating reference frame, the surge can be steadily followed (Fig. 1). The upstream and downstream velocities are respectively V_1 and V_2 and the bore celerity is U. The initial and final water depths are h_1 and h_2. The Froude number based on the initial water elevation is calculated in the moving frame as follows:

$$Fr = \frac{V_1 + U}{\sqrt{g \times h_1}} \quad (1)$$

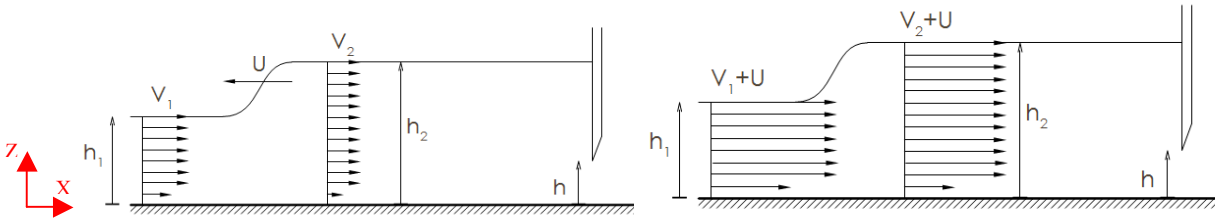

Fig.1: Scheme of the tidal bore viewed in the laboratory and in the translating reference frames

2.2 Experimental set-up

Experiments were performed in a L=8m long and B=0.4m wide flume built with glass walls (Fig. 2). The channel slope is 0% and a constant flow rate up to 60 liters per second (L/s) is ensured by a worm pump. In order to provide an initial flow as smooth and uniform as possible, a 2m long 3D-contraction with a honeycomb grid was positioned upstream. This contraction has progressive vertical and transversal restrictions to limit the development of the vertical and lateral boundary layers. At the end of the flume a reservoir connected to the pump is placed to collect the water.

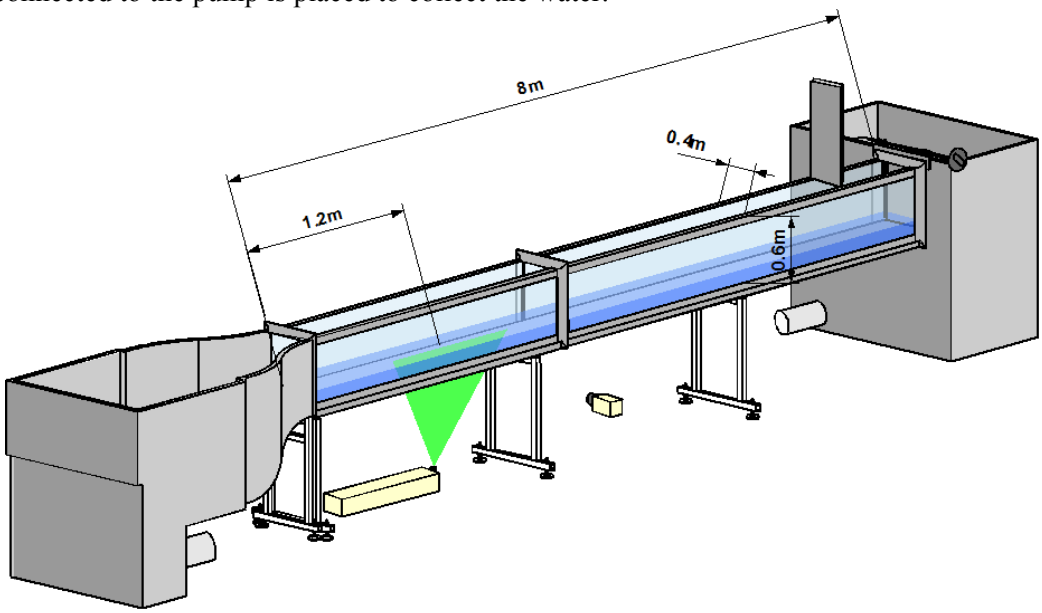

Fig.2: Experimental device of the tidal bore generation.

For the generation of the positive surge into the channel, the pump is started and the flow reaches its equilibrium. Then tidal bores are generated by the rapid partial closure of a sluice gate situated at the downstream end of the flume. The sluice gate is operated from a monitored electro-pneumatic actuator which is also used to trig the acquisition of experimental data, leading to a perfectly reproducible bore generation

procedure. The final gate opening h is adjusted to 35 mm for these experiments, resulting in an overall closing time of 0.1s and a mean gate velocity of 1.25m/s. At the gate closure, the water depth increases and induces a positive surge propagating upstream into the flume (Fig 1). This surge, after an establishment time, leads to a moving bore. The gate was kept close until the acquisition was finished. The generation of the bore is established after 5m and the repeatability of the generation for different Froude numbers, different initial water depths and initial velocities have been validated (David et al., 2014).
For generating three different boundary layers, we used three convergent designs. A 3D convergent suppressed the boundary layers, then a 2D convergent with no vertical constriction allowed the boundary layer development over the flume bed and finally we placed a 100 mm wide band of synthetic grass behind the honeycomb grid to force the transition of the boundary layer (Fig. 3). The flow discharge is fixed to 25 L/s which results in a Froude number of 1.29. This is just where the transition between an undular bore pattern and a breaking bore appears, exhibiting a small roller on the bore front. The upstream velocity profiles are given on Fig.3 for the three convergent designs. For the 3D convergent, a quasi top hat velocity profile is obtained (only 15% of the water depth has a dimensionless velocity lower than one)) whereas a boundary layer profile is generated by the 2D convergent, which is significantly thickened by the synthetic grass tripping. In these two last cases, 25% and 50% of the water depth are respectively affected by the effect of the boundary layer.

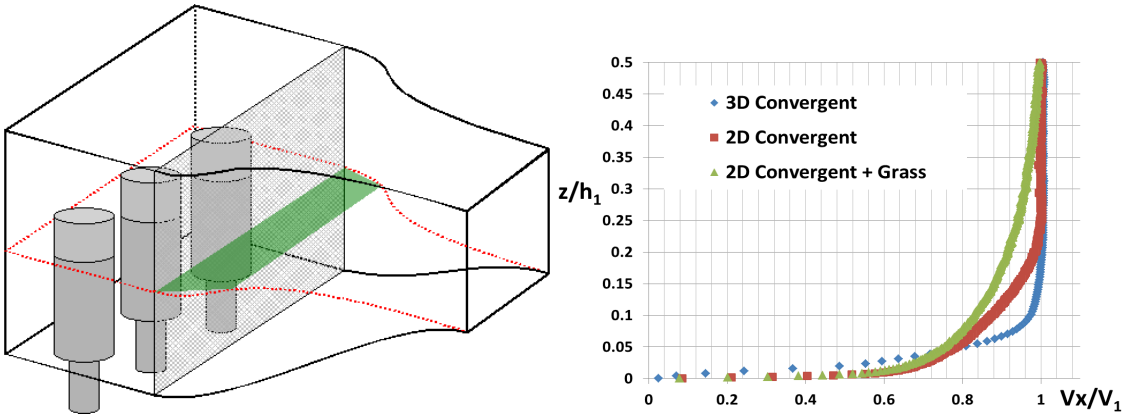

Fig. 3: 2D and 3D convergent designs and upstream velocity profiles with the different boundary layer conditions.

2.3 Data acquisition and processing

The water depth was measured with a series of acoustic displacement meters (Microsonic mic+25/IU/TC) placed at -750, -125, 200, and 750 mm from the center of the PIV field. The accuracy of such sensors is 0.1mm. Both systems were synchronized with the gate closure. Four sensors were used for the validation of the measurements area and for ensuring that the bore is well established and that its velocity is constant in the zone of measurement at 1.2 m to the entrance of the flume.
Velocity measurements were made by a TR-PIV system located at 1200mm from the end of the convergent, to let the surge evolving into a tidal bore (Fig. 2). A 1 mega-pixel fast camera (Photron SA-1) with a 50mm focal lens and a 527nm double pulsed 20mJ Nd:YLFQuantronix® laser with 250 Hz repetition rates were used. The optics were arranged in such way that the laser beam emerged as a planar light sheet perpendicular to the flume wall. The laser sheet was aligned with the center plane of the flume away from the side wall boundary layers. The field of view was a 300mm wide square window. A period of 16 second was recorded; each run was synchronized with the gate motion, providing 4000 images per run.
At the bore front, air bubbles may happen. The reflection of light on those bubbles causes the saturation of the camera sensors. To avoid that, the flow was seeded by 20ìm PMMA particles of density 1.18 doped with Rhodamine-b. The Rhodamine-b wavelength absorption is around 542nm, and, its emission peak is at 565nm. Thus we can bypass the bubble's reflections by using a 540nm high pass filter on the camera's lens.
In order to optimize the PIV image processing, we applied a masking procedure to blacken unnecessary parts due to some reflections close to the free surface. We used the depth signals to cut all parts which were above the water level as well as the channel floor that appears at the bottom of the image. To do that, we first

needed to repair the depth signals because of the loss of signal when the water surface was too steep, reflecting the ultrasonic beam away from the sensor and killing its signal. We fixed it with a linear fit of the slope. Then we could use the signal of the two nearest depth sensors from the center of the PIV field to locate the free surface on the images. The two signals were weighted according to their distance from the position on the picture to gain in accuracy and the mask was created (Fig. 4). Once the images were processed, we used a TR-PIV algorithm (Jeon et al., 2013) based on a sequence of images and an ensemble fluid trajectory correlation (FTEE) to determine vector fields. A sequence of 7 images with a final window size of 32x32 pixels and 75% overlapping is used for the evaluation of a second order polynomial which allows the acceleration estimation during the processing.

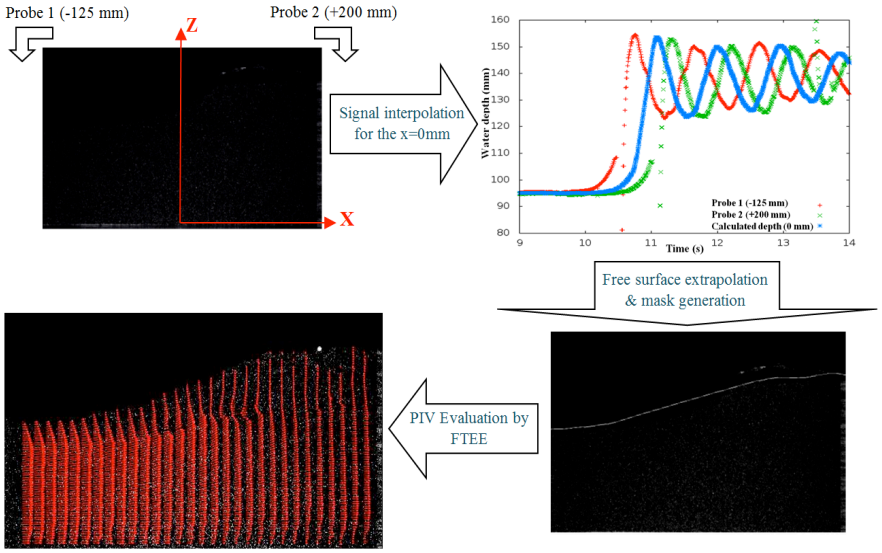

Fig.4: Image processing algorithm for the adaptating mask applied befor the velocity evaluation.

3. Results

3.1 Water depth evolution with the boundary layer conditions

The evaluation of the effect of the boundary conditions on the water depth has been studied for a Froude number of 1.29. The water depths are exactly the same (about 95-96 mm) before the arrival of the bores obtained for the three different flow boundary layer conditions and have the same evolutions and about the same levels during its arrival (Fig. 5). For more clarity, the different signals have been shifted in time to avoid the superposition. After a sudden increase of the water level, the front of the bore is followed by an undular wave which propagates upstream relatively slowly. The suite of well-formed whelps is characterized by its amplitude and its wavelength which don't seem affected by the initial conditions. So the boundary layer of the initial flow for the same Froude number doesn't seem to have a major impact on the tidal bore water level shape. No roller is visible on the water level signal.

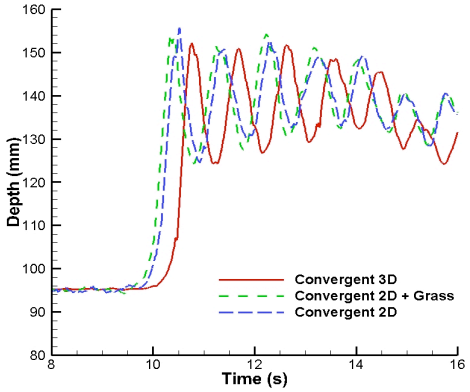

Fig. 5: Water depth evolution for three different boundary layer conditions at Fr=1.29 during the arrival of the bore for h=35 mm.

3.2 Velocity field analysis

Time-resolved velocity measurements allow to observe the flow during the arrival of the bore (Figure 6). Before the arrival of the bore (t=10.2s) we see the distribution of the streamwise component of velocity and the presence of the boundary layer. The bore arrives at t=10.6s and the roller is shown by the negative component in the upper part of the wave. The increase of the water depth during the passage of the bore creates a pressure gradient which allows the development of the boundary layer. At the end of the passage of the wave, the pressure gradient is reversed and the thickness of the boundary layer decreases progressively (t=11s). At the second whelp, the boundary layer thickens again to increase and, along with the decrease of velocity, tends to gradually influence the inner flow pattern (t=11.4s). If we look for the differences between the two different conditions of the boundary layer for the 2D convergent, we see that the expansion of the boundary layer is larger in the case of the more extended initial boundary layer (with grass). The flow seems to be more affected by the turbulence in this case and the velocity increases and decreases in the water column less progressively but more by region. In the case of the less developed boundary layer, the variations of velocity are very progressive during the passage of the bore (Figure 7).
Close to the bottom, the boundary layer thickness seems to be very influential on the flow. No inversion of the flow is observed in this case (some other experiments for different flow conditions and Froude numbers have revealed a brief inversion of the flow) but when the boundary layer is larger, some vortices appear along the flume bed during the passage of the different whelps. The most intense vortex structure appears for the first water raise but others occur for the successive whelps in the case of a 2D contraction with grass tripping.

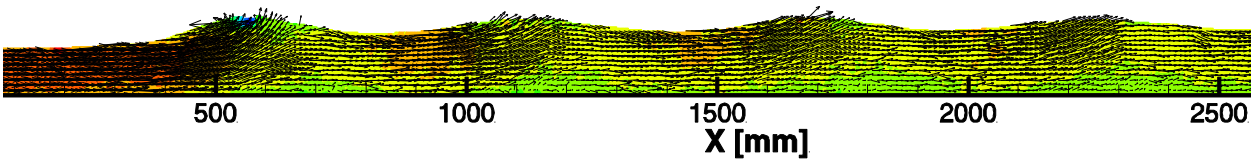

Fig. 7: Reconstruction of the time evolution of the bore in the X direction for the 3D convergent initial condition.

4. Conclusion

Positive surges have been studied in laboratory using TR-PIV and water depth measurements. Some adaptation of the PIV has been introduced to be able to measure the flow for different kind of bores. Particles doped with Rhodamine and adaptative masking calculated from acoustic sensors to mark the free surface have been used to improve the velocity estimation in an open channel flow. Various kinds of translating bores have been studied in a laboratory flume in order to allow the understanding of the development and of the time evolution of tidal bores in natural conditions. An undular bore close to the transition (Fr=1.29) has been generated for several initial boundary layer conditions. This parameter doesn't seem to affect the free surface time evolution while it appears essential inside the water column for the turbulence development and the mixing of the boundary layer with the inertial sub layer. The time evolution of the velocity fields will help a better description of the flow during the passage of such bores and will improve the understanding of this phenomenon.

Acknowledgments

The authors would like to acknowledge the French National Agency for their financial support in the Project BLANC MASCARET 10-BLAN-0911, the FEDER and the Region Poitou Charentes. Professor L. David would also like to thank Professor H. Chanson for their fruitful discussions during the summer 2011.

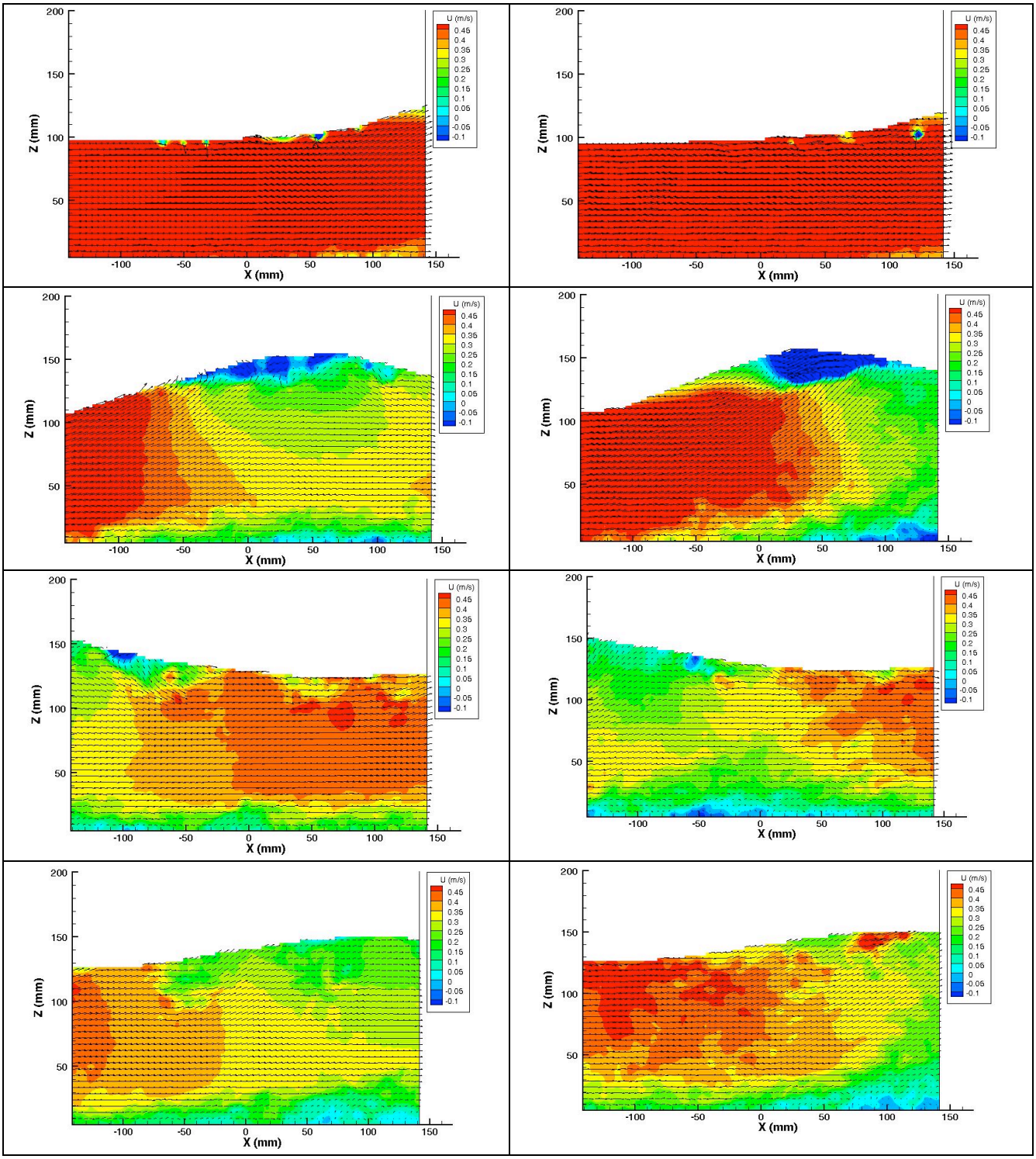

Fig.6:Velocity fields and streamwise velocity during the passage of the positive surge for different times (t=10.2, 10.6,11, 11.4s since the generation t=0s) left 2D convergent, right 2D convergent with grass.

References

Barré de Saint-Venant, A.J.C. (1871). Théorie et équations générales du mouvement non permanent des eaux courantes. *Comptes Rendus des séances de l'Académie des Sciences*, Paris, France, Séance 17 July 1871, 73, 147–154 (in French).

Benjamin, T. B., Lighthill, M. J. (1954). On Cnoidal waves and bores.*Proc. R. Soc. London. Set: A*, 224(

1159), 448-460.
Chanson, H. (2010).Undular Tidal Bores: Basic Theory and Free-surface Characteristics. *Journal of Hydraulic Engineering*, 136 (11), 940-944 (DOI: 10.1061/(ASCE)HY.1943-7900.0000264).
Chanson, H. (2011). Tidal Bores, Aegir, Eagre, Mascaret, Pororoca: Theory and Observations. *World Scientific,* Singapore (ISBN 9789814335416).
Chanson H., Docherty N. J., (2012). Turbulent velocity measurements in open channel bores. European *Journal of Mechanics B/Fluids* 32, 52–58.
David L., Lebon B., Chatellier L., Calluaud D., (2012).Influence of initial flow boundary conditions on undular tidal bores. *3rd IAHR Europe Congress*, 2014, Porto (Portugal).
HornungHG.,Willert C., and Turner S., 1995. The flow field downstream of a hydraulic jump.*J. Fluid Mech*, Vol 287, pp. 299-316.
Huang J., Pan CH, Kuang CP, Zeng J, Chen G, (2013). Experimental hydrodynamic study of the Qiantang River tidal bore. *Journal of Hydrodynamics*, 25(3):481-490
Jeon Y. J., Chatellier L., and David L. (2013).Evaluation of fluid trajectory in time-resolved piv.*10th International Symposium on Particle Image Velocimetry* – PIV 13, Delft, The Netherlands.
Jian S., Chaofeng T., Yixin Yan, Xingqi L.(2014) Influence of varying shape and depth on the generation of tidal bores. *Environ Earth Sci*.
Koch C., Chanson H., (2009). Turbulence measurements in positive surges and bores.*Journal of Hydraulic Research* Vol. 47, No. 1, pp. 29–40.
Lemoine R, (1948). Sur le sondes positives de translation dans les canaux et sur le ressaut ondulé de faible amplitude. *La Houille Blanche*, 183-185
Lubin P., Chanson H., Glockner S., (2010).Large Eddy Simulation of turbulence generated by a weak breaking tidal bore. *Environ Fluid Mech*, 10:587–602.
Tessier B., and Terwindt, J. H. J. (1994). An example of soft sediment deformations in an intertidal environment: the effect of a tidal bore. Comptes Rendus—Academie des Sciences, Serie II, 319, 217–223.
Wolanski, E., Williams, D., Spagnol, S., and Chanson H. (2004).Undular tidal bore dynamics in the daly estuary, northern australia. Estuarine Coastal Shelf Science, 60, 629–636.
Xie D.F., Pan C.H., (2013) A preliminary study of the turbulence features of the tidal bore in the Qiantang River, China. *Journal of hydrodynamics* 25(6):903-911